Supporting Information

Aqueous, Heterogeneous Parahydrogen-Induced ^{15}N Polarization

Liana B. Bales,[a] Kirill V. Kovtunov,[b,c,*] Danila A. Barskiy,[g] Roman V. Shchepin,[g] Aaron M. Coffey,[g] Larisa M. Kovtunova,[c,d] Andrey V. Bukhtiyarov,[d] Matthew Feldman,[g] Valerii I. Bukhtiyarov,[c,d] Eduard Y. Chekmenev,[e,f,g,*] Igor V. Koptyug,[b,c] Boyd M. Goodson[a,h,*]

[a]Department of Chemistry and Biochemistry, [h]Materials Technology Center, Southern Illinois University, Carbondale, IL 62901, USA
[b]International Tomography Center SB RAS, Novosibirsk, 630090, Russia
[c]Novosibirsk State University, Novosibirsk, 630090, Russia
[d]Boreskov Institute of Catalysis SB RAS, Novosibirsk, 630090, Russia
[e]Department of Biomedical Engineering and Physics, Vanderbilt-Ingram Cancer Center (VICC), [g]Vanderbilt Institute of Imaging Science (VUIIS), Department of Radiology, Vanderbilt University Medical Center, Nashville, TN 37232, USA
[f]Russian Academy of Sciences, Moscow, 119991, Russia

1. Catalyst Preparation

Two different Rh/TiO_2 catalysts, one with 1.0 wt% and the second with 23.2 wt% metal loading, were prepared using the wet impregnation technique. The TiO_2 powder (Hombifine N, S_{BET} = 107 m^2/g) was calcinated at 500 °C for 2 hours prior to use.

During the preparation of Rh/TiO_2 catalyst with 1.0 wt% metal loading, the acidic solution of $Rh(NO_3)_3$ with a metal concentration of 38 mg/ml was used. A 0.53 ml of $Rh(NO_3)_3$ solution was diluted in water until a total volume of 1.6 ml was obtained. Then, 2 g of TiO_2 was impregnated with the aqueous solution of rhodium for 1 hour at room temperature. The solvent excess was evaporated and the formed catalyst was air dried at 120 °C for 4 hours. The next calcination of the samples was performed at 400 °C in air for 3 hours with subsequent reduction of samples in H_2 flow at 330 °C for 3 hours.

During the preparation of Rh/TiO_2 catalyst with 23.2 wt% metal loading, the acidic solution of $Rh(NO_3)_3$ with a metal concentration of 98 mg/ml was used. Here, 6.1 ml of $Rh(NO_3)_3$ solution was evaporated to dryness and diluted with water to obtain a total volume of 2 ml, after which 5 drops of 25% tetramethylammonium hydroxide in water (Acros, CAS:75-59-2) were added. Then, 2 g of TiO_2 was impregnated with the aqueous solution of rhodium for 2.5 hours at room temperature. The solvent excess was evaporated and the formed catalyst was air dried at 120 °C for 4 hours. The next calcination of the sample was done at 400 °C in air for 3 hours with subsequent reduction of the sample in H_2 flow at 330 °C for 3 hours.

2. Synthesis of ^{15}N-labeled Molecules

Preparations were performed using Renshaw's adaptation[1] of the Bode[2] method.

Synthesis of Neurine-^{15}N-d_3 Bromide

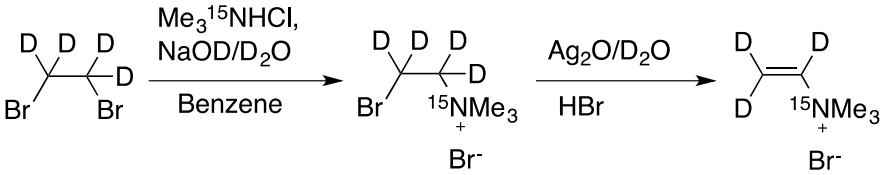

Figure S1. Reaction scheme for synthesis of neurine-^{15}*N*-d_3 bromide from trimethylamine-^{15}*N* hydrochloride.

Trimethylamine-^{15}*N* hydrochloride (1.00 g, 10.0 mmol) was placed in a 10 ml vial and dissolved in D_2O (2 ml). The solution was transferred via syringe to a thick glass 15 ml ampoule and the vial was washed with additional D_2O (1 ml). The ampoule (1/8" x 6") was cooled to -78 °C until the solution inside completely froze. 1,2-dibromoethane-d_4 (5.00 g, 26.0 mmol) dissolved in benzene (7 ml) was added slowly to the cooled ampoule. NaOD (40% solution in D_2O, 1.08 g, 10.5 mmol) was dilute in a vial with D_2O (1 ml) and the solution was transferred in the ampoule on top of the frozen benzene layer. Once the contents of the entire ampoule were completely frozen, the ampoule was sealed and left to thaw at room temperature. After a week, the solution was gently mixed by flipping the ampoule and it was left for two more weeks. The ampoule was opened, its contents were transferred to a round bottom flask, and they were then washed with additional D_2O (10 ml). The combined solution was evaporated to dryness under reduced pressure (<1 mbar) for 2 hours, producing crude bromocholine-^{15}*N*-d_4 bromide.

Silver oxide was prepared fresh. First, $AgNO_3$ (4.25 g, 25.0 mmol) was dissolved in water (25 ml) and it was cooled to 0°C. NaOH (1.00 g, 25.0 mmol) in water was added dropwise and the resulting gray suspension was gently stirred using a magnetic stirrer for 20 min. After that, silver oxide was collected on a Buchner funnel and was washed with water and D_2O.

Bromocholine-^{15}*N*-d_4 bromide was dissolved in D_2O (20 ml) and Ag_2O was added in small portions. After 30 min., it was filtered and the liquid phase was concentrated in vacuo at 30°C for 1 hour. The oily residue was dissolved in water and HBr (48% in H_2O) was added until pH<0. The solution was dried under reduced pressure and the product was recrystallized from ethanol/diethyl ether, furnishing *N*eurine-^{15}*N*-d_3 bromide (1.33 g, 78%).

Synthesis of Neurine-^{15}N-d_{12} Bromide

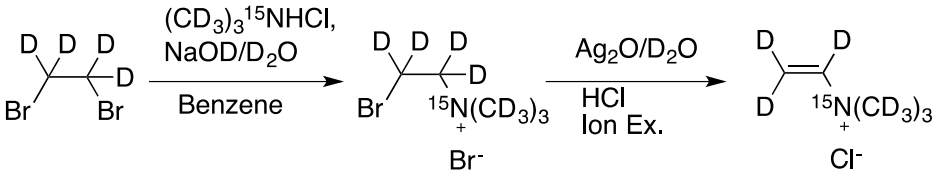

Figure S2. Reaction scheme of synthesizing neurine-^{15}N-d_{12} chloride from trimethylamine-^{15}N,d_9 hydrochloride.

Trimethylamine-^{15}N-d_9 hydrochloride (0.5 g, 4.7 mmol) was placed in a 10 ml vial and dissolved in D_2O (1 ml). The solution was transferred via syringe to a thick glass 15 ml ampoule and the vial was washed with additional D_2O (1 ml). The ampoule (1/8" x 6") was cooled to -78°C until the solution completely froze. 1,2-dibromoethane-d_4 (5.00 g, 26.0 mmol) dissolved in benzene (7 ml) was added slowly to the cooled ampoule. Then, NaOD (40% solution in D_2O, 0.50 g, 4.9 mmol) was diluted in a vial with D_2O (0.5 ml) and the solution was transferred in the ampoule on top of the frozen benzene layer. While the entire ampoule content was completely frozen, it was sealed and left to thaw at room temperature. After a week, the solution was gently mixed by flipping the ampoule and it was left for two more months. The ampoule was opened, and its contents were transferred to a round bottom flask, and they were washed with additional D_2O (10 ml). The combined solution was evaporated to dryness under reduced pressure (<1 mbar) for 2 hours. The residue was washed with ether, producing crude bromocholine-^{15}N-d_{13} bromide.

Silver oxide was prepared fresh. First, $AgNO_3$ (2.12 g, 12.5 mmol) was dissolved in water (14 ml) and it was cooled to 0°C. NaOH (0.50 g, 12.5 mmol) in water (5 ml) was added dropwise and the resulting gray suspension was gently stirred using a magnetic stirrer for 20 min. After that, silver oxide was collected on a Buchner funnel and was washed with water and D_2O.

Bromocholine-^{15}N-d_{13} bromide was dissolved in D_2O (20 ml) and Ag_2O was added in small portions. After 30 min., the solution was filtered and the liquid phase was concentrated in vacuo at 30°C for 1 hour. It was then redissolved in D_2O (20 ml) and evaporated again. The oily residue was dissolved in water and HCl (37% in H_2O) was added until pH<0. Next, the solution was dried under reduced pressure.

An ion-exchange column was prepared from exchange Amberlite IRA-400 (~75 ml) beads) by running H_2O through it (200 ml). Neurine-^{15}N-d_{12} bromide was dissolved in several ml of H_2O and was run through the column, eluting rapidly within the first 80

ml. It was concentrated, re-dissolved in absolute ethanol twice, and evaporated in order to remove traces of water. The product was pure, but it was recrystallized from ethanol/THF (5:40 ml), yielding 0.341 g of product.

Synthesis of Neurine-^{15}N Bromide

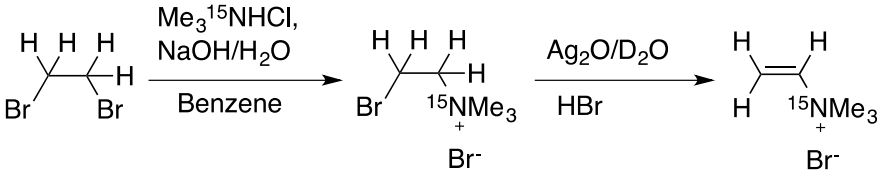

Figure S4. Reaction scheme of synthesizing neurine-^{15}N bromide from 1,2-dibromoethane.

Neurine-^{15}N bromide was prepared in the same manner as ^{15}N-d_3-neurine bromide (described above, following the Renshaw method[1]), starting from 1,2-dibromoethane. The final product contained ~4% of 1,2-di(trimethylammonium-^{15}N)ethane dibromide.

3. Sample Preparation and Aqueous Phase Heterogeneous Hydrogenation of ^{15}N-labeled Molecules

For the aqueous phase heterogeneous hydrogenation of neurine-^{15}N bromide aqueous solution, 2.4 ml of D_2O was premixed with 100 (or 50 for the results presented in Figure 2 of the main text) mg of neurine-^{15}N bromide. The resulting 0.25 M (or 0.125 M for Figure 2) solution (0.5 ml) was placed in a medium wall 5 mm NMR tube with 10 mg of Rh/TiO_2 catalysts placed at the bottom. The NMR tube was heated to ~90 °C. The hydrogenation was performed with a p-H_2 pressure of ~7.1 atm and a flow rate of 100 standard cubic centimeters per minute (sccm) controlled by the mass-flow controller. For the polarization transfer experiments, the field cycling approach with a magnetic shield was used. The full experimental setup is shown in Figure S5. The detailed information about the setup, polarization transfer procedure, and magnetic field strength are given in references.[3,4]

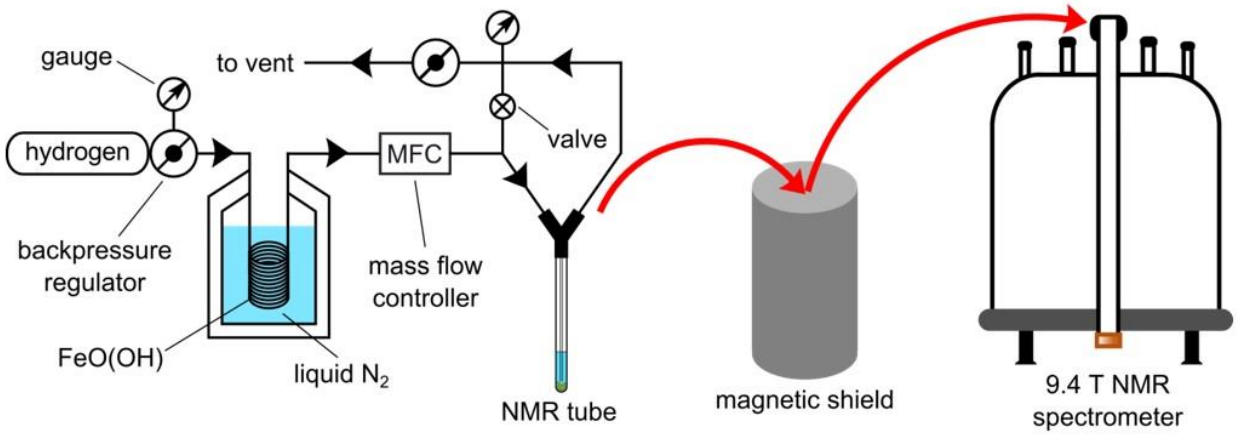

Figure S5. Experimental setup for aqueous phase heterogeneous hydrogenation with polarization transfer to ^{15}N nuclei using magnetic field cycling.

4. Low-Field Instrumentation

Our experimental low field NMR apparatus is comprised of a 0.049 T permanent magnet. It has an 80 cm bore width and has a homogeneity of ~50 ppm across a 400 mm DSV (diameter of spherical volume) which corresponds to a 25 Hz ^{1}H spectral linewidth (FWHM, full width half max). The magnet homogeneity was achieved using Neodymium shim magnets in five sizes. The homogeneity can be improved marginally by driving a DC offset current through three orthogonal magnetic gradients. The console used to control the NMR system is a Tecmag Redstone system, which has three receiver and transmitter channels operable across a bandwidth from 0.1-3 MHz. The nominal noise figure of the receivers is 1.5 dB.

The RF coils for this system were built to measure samples stored in standard 5 and 10 mm diameter NMR tubes. To increase the SNR, a solenoid coil matching the dimensions of the NMR sample (17 mm diameter by 193 mm) was built, thereby improving the filling factor of the coil. The quality factor of the coil was 70. The coil was tuned using ATC nonmagnetic ceramic capacitors and two Johansen trimmer capacitors to tune the center frequency and the power match of the coil. The circuit design was a parallel LC resonator with a series capacitive matching element. The solenoid had 878 windings using 0.22 mm diameter wire with a measured inductance of 839.6 μH. The coil was calibrated using a nutation sequence and its 90° tip angle was found to be 500 μs. Each coil winding was directly adjacent to its nearest neighbor winding, which led to additional capacitance contribution to the LC parallel resonator. The coil was shielded from electric field interference and noise by housing it in a hollow copper cube made out of square copper clad PCB materials (1 ft x 1 ft). A circular waveguide 50 mm in

length was built to protrude from the shield to act as an access point for the sample to be inserted into the coil. The shielding provided an electric field suppression of 60 dB.

5. Parahydrogen

A home-built system was used to produce parahydrogen (p-H_2) gas for the liquid-phase heterogeneous hydrogenation experiments involving the neurine-^{15}N bromide aqueous solutions. This system enriches room temperature bulk H_2 (close to 75% *ortho*- and 25% *para*-state at Boltzmann equilibrium for this spin temperature) with an increased p-H_2 fraction. The permissible flow rate ranges from 0 to 150 sccm, which may be attained at outlet pressures ranging from 0 to 25 bar gauge pressure. The catalyst used for *ortho*- to *para*- state conversion of bulk H_2 was FeO(OH) 30-50 mesh catalyst (SKU 371254-50G, Sigma-Aldrich). Approximately 3 g of this catalyst was packed inside a sealed chamber affixed to the cold finger of a single-stage cryocooler (CryoTel, Sunpower Inc, Athens, OH). A continuous production rate and purity of p-H_2 (i.e. steady-state conditions) was attained through use of a mass flow controller (MFC) (Sierra Instruments, Monterey, CA, model no. C100L-DD-OV1-SV1-PV2-V1-S0-C0) to regulate the flow rate. In particular, the MFC ensures that the bulk H_2 gas heat transfer and the energy of conversion[5] from orthohydrogen (o-H_2) to p-H_2 does not overwhelm the cooling capacity of the cryocooler.

The home-built system produced p-H_2 of ~80% purity. The level of purity was assessed by high-field NMR at 9.4 T using an experimental setup first devised[6] and later described in detail[7] for SABRE experiments, which allows faster measurements of p-H_2 quality than our earlier reported method[8] involving waiting for in-tube relaxation back to room temperature equilibrium (i.e. 75% *ortho*-state). Briefly, in this experimental setup a 5 mm NMR tube residing in the 9.4 T NMR magnet is connected with ¼ in. Teflon tubing to a wye push-to-connect tube fitting (p/n 5779K262, McMaster-Carr). One port of the wye connector serves as exhaust, and the other is alternately connected to either bulk H_2 or to a p-H_2 source. The signal level from bulk H_2 was first obtained and its integral calibrated according to the presence of 75% o-H_2. Next, p-H_2 from the home-built system was connected and measured using the bulk H_2 signal level as a reference. The measured purity of the p-H_2 as obtained by this method (~80%) was found to agree quantitatively (within < 1%) with the cold-finger temperature of the cryocooler of ~48 K.

6. Catalyst Characterization

X-Ray Photoelectron Spectroscopy

The XPS measurements of samples was performed on a SPECS (Germany) photoelectron spectrometer equipped with a PHOIBOS-150 hemispherical energy analyzer and AlK_α irradiation (hν=1486.6 eV, 200 W). The binding energy (BE) scale was pre-calibrated using the positions of the photoelectron of $Au4f_{7/2}$ (BE=84.0 eV) and $Cu2p_{3/2}$ (BE=932.67 eV) core level peaks.

The binding energy of peaks was calibrated by the position of the Ti2p peak (BE=458.8 eV) corresponding to the Ti^{4+} from the TiO_2. It should be mentioned that the loading process never exceed 1 min. in order to minimize the sample contact with air. Spectral analysis and data processing were performed with XPS Peak 4.1 program.[9] For quantitative analysis, integral intensities of the spectra collected (Ti2p, C1s, O1s, Br3d and Rh3d) using the SPECS spectrometer were corrected by their respective atomic sensitivity factors.[10]

The ratios of elements atomic concentrations calculated from XPS data are presented in Table S1. For the sample measured after reaction, the Rh/Ti atomic ratio decreased along with the increase of C/Rh ratio. At the same time the C/Ti atomic ratio increased just slightly. Additionally the appearance of the Br3d signal was obtained.

Table S1. Atomic ratios of elements calculated from XPS data

Sample	Rh/Ti	C/Ti	O/Ti	OH^-/O^{2-}	Br/Ti	C/Rh
Fresh	0.023	1.5	2.29	0.09	0	66.2
After reaction	0.012	1.6	2.31	0.11	0.11	136.3

Figure S6 presents Rh3d (left panel) and C1s (right panel) core-level spectra obtained for the fresh Rh/TiO_2 catalyst and after reaction. The $Rh3d_{5/2}$ peak at 307.4 eV measured for the fresh sample can be attributed to metallic Rh (Rh^0).[10,11] One can see the shift of the $Rh3d_{5/2}$ peak position to lower binding energy (307.0 eV) for the sample measured after reaction. This shift could be attributed to a sample surface conductivity change induced by the carbonization of the surfaces of the Rh nanoparticles.

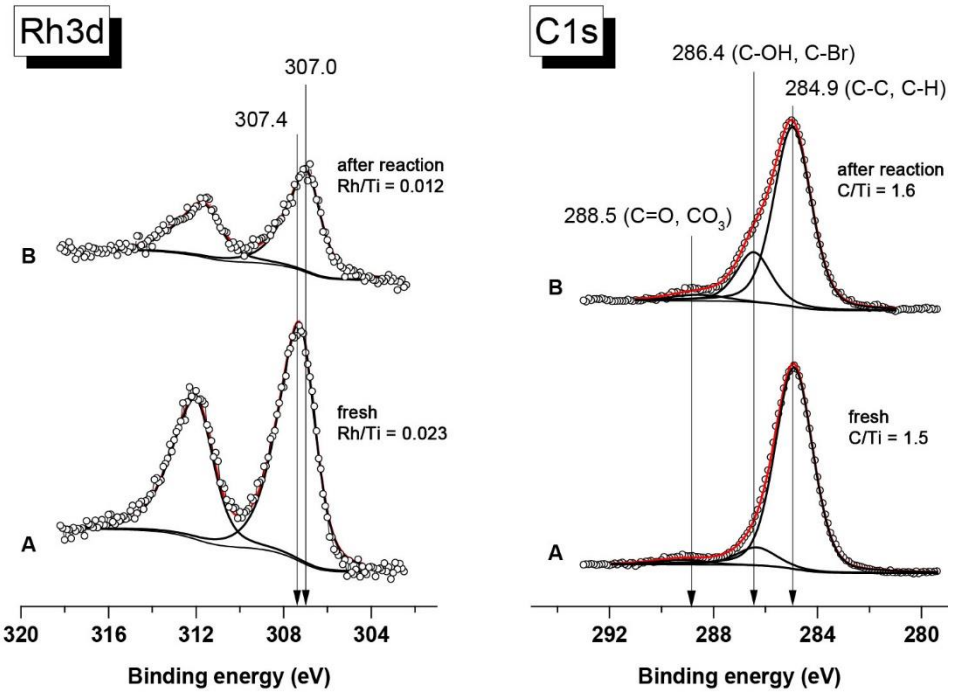

Figure S6. XPS spectra of Rh3d (left panel) and C1s (right panel) measured for (A) fresh Rh/TiO_2 and (B) Rh/TiO_2 after reaction.

From the C1s spectra (Fig. S6 right panel) one can see that three-carbon species with different binding energies are presented at the surface. The most intense peak (corresponding to a binding energy of 284.9 eV) is typical to the surface hydrocarbon atoms (C=C and C–H bonds).[10,12] The species at 286.4 eV could be attributed to C-OH or C-Br bonds.[13,14,15] The C1s peaks with higher binding energies (~288.5 eV) can usually be attributed to the carboxyls/carbonates carbon species.[10] Oxygen in O1s core-level spectra presented as two species with binding energies of 530.1 and 531.6 eV, which were assigned according to literature data to lattice oxygen Ti-O-Ti and surface Ti-OH groups, respectively.[16,17] It should be noted that the atomic ratio between these oxygen species (OH^-/O^{2-}) is almost the same for the surface measured before and after reaction (see Table S1).

Figure S7 presents Br3d core-level spectra region obtained for the fresh Rh/TiO_2 catalyst and after reaction. The Br3d signal appearance for the sample measured after reaction was obtained. The Br presented only in one state with a binding energy of 68.4 eV, which is typical for the Br^- species.[18,19]

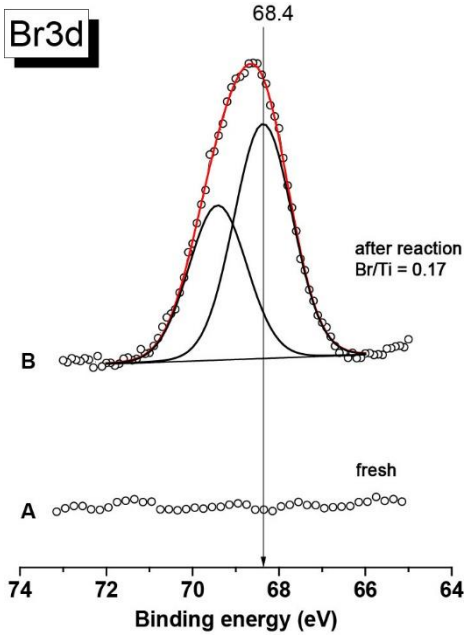

Figure S7. XPS spectra of Br3d measured for (A) fresh Rh/TiO_2 and (B) Rh/TiO_2 after reaction.

7. Additional NMR Spectra

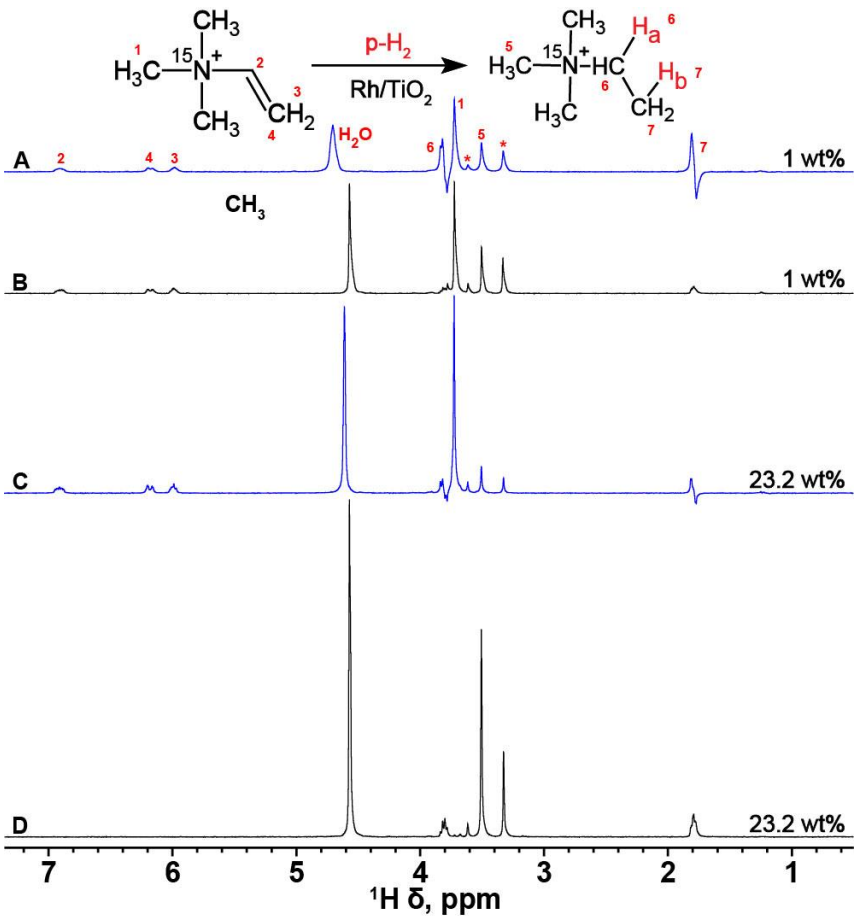

Figure S8. Single shot ^{1}H NMR spectra, referenced to spectrum A. (A) Hydrogenation of ^{15}N-trimethyl(vinyl)-ammonium (neurine-*^{15}N*) bromide in the presence of 1% Rh/TiO_2 in the PASADENA regime[20] after 30 seconds of bubbling, leading to transfer of ^{1}H spin order at the nascent H sites on the ^{15}N-ethyl trimethyl ammonium ion product. (B) After ~45 seconds of p-H_2 bubbling, but also after sufficient time to allow signal relaxation, in the presence of 1% Rh/TiO_2. (C) Hydrogenation of ^{15}N-trimethyl(vinyl)ammonium bromide in the presence of 20% Rh/TiO_2 in the PASADENA regime after 5 seconds of bubbling, leading to transfer of ^{1}H spin order at the nascent H sites on the ^{15}N-ethyl trimethyl ammonium ion product. (D) After ~45 seconds of p-H_2 bubbling, but also after sufficient time to allow signal relaxation, in the presence of 20% Rh/TiO_2; under these conditions, full conversion of the substrate to the saturated product is observed. All spectra were taken at 90 °C.

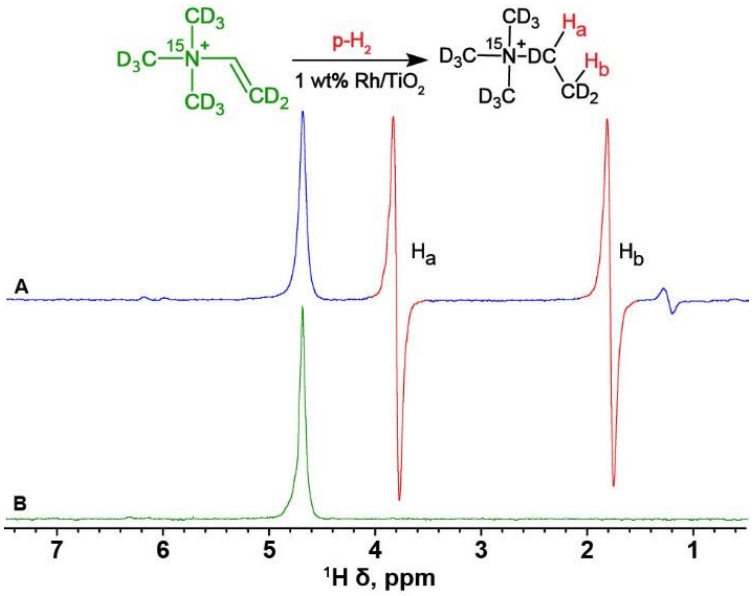

Figure S9. ^{1}H NMR spectra of the fully deuterated substrate (A) during hyperpolarization / hydrogenation in the PASADENA regime; and (B) before reaction.

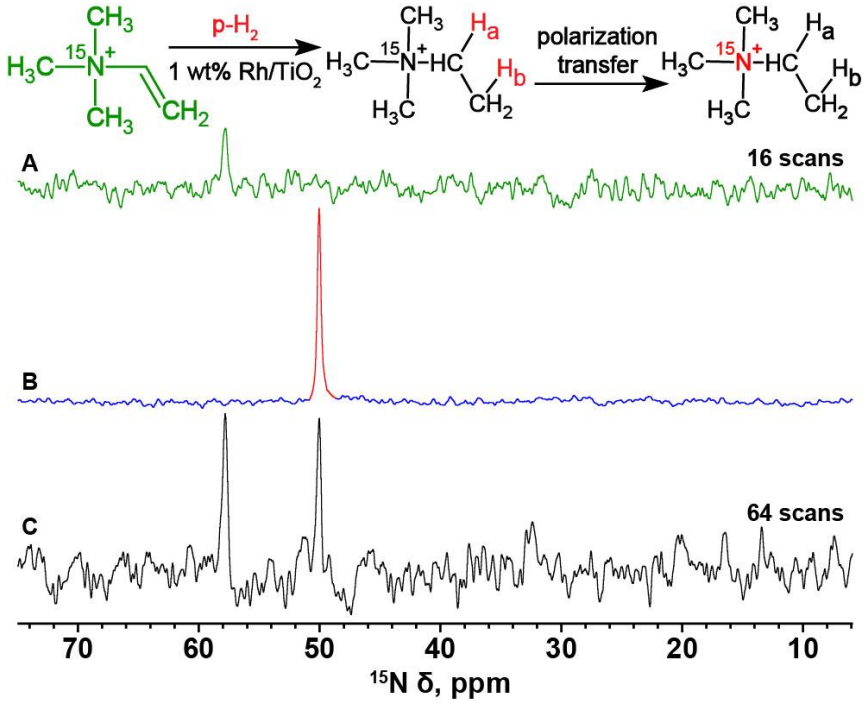

Figure S10. ^{15}N NMR spectra in the presence of 1% Rh/TiO_2 (referenced to spectrum A). (A) Before reaction taken with 16 scans at a concentration of 0.125 M, showing relative ^{15}N shift of reactant. (B) ^{15}N HET-PHIP resulting in hyperpolarization of ^{15}N-ethyl trimethyl ammonium ion following 30 s of p-H_2 bubbling (note the chemical shift difference of the product). (C) Non-hyperpolarized spectrum taken after 2 minutes, 30 seconds p-H_2 bubbling, but also after signal relaxation occurred (30 s recycle delay), showing reaction progress at that point.

References Used in Supporting Information

(1) Renshaw, R. R. Some Derivatives of Choline: [Second Paper]. *J. Am. Chem. Soc*. **1912**, *34*, 1615–1619.
(2) Bode, J. Ueber Einige Abkömmlinge des Neurins und Cholins. *Justus Liebigs Ann. Chem*. **1892**, *267*, 268–299.
(3) Theis, T.; Truong, M. L.; Coffey, A. M.; Shchepin, R. V.; Waddell, K. W.; Shi, F.; Goodson, B. M.; Warren, W. S.; Chekmenev, E. Y. Microtesla SABRE Enables 10% Nitrogen-15 Nuclear Spin Polarization. *J. Am. Chem. Soc*. **2015**, *137*, 1404–1407.
(4) Shchepin, R. V.; Barskiy, D. A.; Coffey, A. M.; Manzanera Esteve, I. V.; Chekmenev, E. Y. Efficient Synthesis of Molecular Precursors for Para-Hydrogen-Induced Polarization of Ethyl Acetate-1-^{13}C and Beyond. *Angew. Chem. Int. Ed*. **2016**, *55*, 6071–6074.
(5) Hövener, J. B.; Bar, S.; Leupold, J.; Jenne, K.; Leibfritz, D.; Hennig, J.; Duckett, S. B.; von Elverfeldt, D. A Continuous-Flow, High-Throughput, High-Pressure Parahydrogen Converter for Hyperpolarization in a Clinical Setting. *NMR Biomed*. **2013**, *26*, 124–131.
(6) Theis, T.; Truong, M.; Coffey, A. M.; Chekmenev, E. Y.; Warren, W. S. LIGHT-SABRE Enables Efficient in-Magnet Catalytic Hyperpolarization. *J. Magn. Reson*. **2014**, *248*, 23–26.
(7) Truong, M. L.; Theis, T.; Coffey, A. M.; Shchepin, R. V.; Waddell, K. W.; Shi, F.; Goodson, B. M.; Warren, W. S.; Chekmenev, E. Y. ^{15}N Hyperpolarization by Reversible Exchange Using SABRE-SHEATH. *J. Phys. Chem. C* **2015**, *119*, 8786–8797.
(8) Feng, B.; Coffey, A. M.; Colon, R. D.; Chekmenev, E. Y.; Waddell, K. W. A Pulsed Injection Parahydrogen Generator and Techniques for Quantifying Enrichment. *J. Magn. Reson*. **2012**, *214*, 258–262.
(9) http://xpspeak.software.informer.com/4.1/.
(10) Moudler, J.; Stickle, W.; Sobol, P.; Bomben, K. Handbook of X-ray Photoelectron Spectroscopy, Perkin-Elmer Corp.: Eden Prairie, MN, 1992.
(11) Larichev, Y. V.; Netskina, O. V.; Komova, O. V.; Simagina, V. I. Comparative Xps Study of Rh/Al_2O_3 and Rh/TiO_2 as Catalysts for $NaBH_4$ Hydrolysis. *Int. J. Hydrogen Energy* **2010**, *35*, 6501–6507.
(12) Oltedal, V. M.; Børve, K. J.; Sæthre, L. J.; Thomas, T. D.; Bozek, J. D.; Kukk, E. Carbon 1s Photoelectron Spectroscopy of Six-membered Cyclic Hydrocarbons *Phys. Chem. Chem. Phys*. **2004**, *6*, 4254–4259.
(13) Zhang, N.; Zhao, C.; Ma, W.; Wang, S; Wang, B.; Zhang, G.; Li, X.; Na, H. Macromolecular Covalently Cross-linked Quaternary Ammonium Poly(Ether Ether Ketone) with Polybenzimidazole for Anhydrous High Temperature Proton Exchange Membranes. *Polym. Chem*. **2014**, *5*, 4939–4947.
(14) Actis, P.; Caulliez, G.; Shul, G.; Opallo, M.; Mermoux, M.; Marcus, B.; Boukherroub, R.; Szunerits, S. Functionalization of Glassy Carbon with Diazonium Salts in Ionic Liquids. *Langmuir* **2008**, *24*, 6327-6333.
(15) Geng, Z.; Lin, Y.; Yu, X.; Shen, Q.; Ma, L.; Li, Z.; Pan, N.; Wang, X. Highly Efficient Dye Adsorption and Removal: a Functional Hybrid of Reduced Graphene Oxide–Fe_3O_4 Nanoparticles as an Easily Regenerative Adsorbent. *J. Mater. Chem*. **2012**, *22*, 3527–3535.
(16) Li, L.; Yan, J.; Wang, T.; Zhao, Z.-J.; Zhang, J.; Gong, J.; Guan, N. Sub-10 nm Rutile Titanium Dioxide Nanoparticles for Efficient Visible-Light-Driven Photocatalytic Hydrogen Production. *Nat. Commun*. **2015**, *6*, 5881.
(17) Spende, A.; Sobel, N.; Lukas, M.; Zierold, R.; Reidl, J. C.; Gura, L.; Schubert, I.; Moreno, J. M. M.; Nielsch, K.; Stühn, B.; et al. TiO_2 , SiO_2 , and Al_2O_3 Coated Nanopores and Nanotubes Produced by ALD in Etched Ion-Track Membranes for Transport Measurements. *Nanotechnology* **2015**, *26*, 335301–335311.

(18) Li, J.; Xie, Y.; Zhong, Y.; Hu, Y. Facile Synthesis of Z-scheme Ag_2CO_3/Ag/AgBr Ternary Heterostructured Nanorods with Improved Photostability and Photoactivity. *J. Meter. Chem*. A **2015**, *3*, 5474–5481.
(19) Xiong, J.; Dong, Q.; Wang, T.; Jiao, Z.; Lu, G.; Bi, Y. Self-assembled Synthesis of Hierarchical Zn_2GeO_4 Core–shell Microspheres with Enhanced Photocatalytic Activity. *RSC Adv*. **2014**, *4*, 583–586.
(20) Bowers, C. R.; Weitekamp, D. P. Para-Hydrogen and Synthesis Allow Dramatically Enhanced Nuclear Alignment. *J. Am. Chem. Soc.* **1987**, *109*, 5541–5542.